ACS OMEGA

Article

http://pubs.acs.org/journal/acsodf

Systematic Functional Analysis of Active-Site Residues in L-Threonine Dehydrogenase from *Thermoplasma volcanium*

Morgan Desjardins,[†] Wai Shun Mak,[†] Terrence E. O'Brien,[†] Dylan Alexander Carlin,[†] Dean J. Tantillo,[†] and Justin B. Siegel*[,†,‡,§]

[†]Department of Chemistry, University of California, Davis, One Shields Avenue, Davis, California 95616, United States

[‡]Department of Biochemistry and Molecular Medicine, University of California, Davis, 2700 Stockton Boulevard, Suite 2102, Sacramento, California 95817, United States

[§]Genome Center, University of California, Davis, 451 Health Sciences Drive, Davis, California 95616, United States

Supporting Information

ABSTRACT: Enzymes have been through millions of years of evolution during which their active-site microenvironments are fine-tuned. Active-site residues are commonly conserved within protein families, indicating their importance for substrate recognition and catalysis. In this work, we systematically mutated active-site residues of L-threonine dehydrogenase from *Thermoplasma volcanium* and characterized the mutants against a panel of substrate analogs. Our results demonstrate that only a subset of these residues plays an essential role in substrate recognition and catalysis and that the native enzyme activity can be further enhanced roughly 4.6-fold by a single point mutation. Kinetic characterization of mutants on substrate analogs shows that L-threonine dehydrogenase possesses promiscuous activities toward other chemically similar compounds not previously observed. Quantum chemical calculations on the hydride-donating ability of these substrates also reveal that this enzyme did not evolve to harness the intrinsic substrate reactivity for enzyme catalysis. Our analysis provides insights into connections between the details of enzyme active-site structure and specific function. These results are directly applicable to rational enzyme design and engineering.

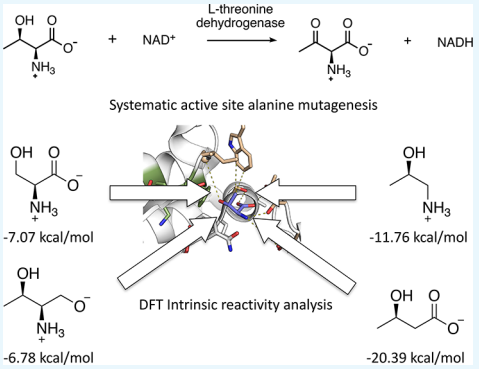

INTRODUCTION

Enzymes have active sites where a myriad of functional groups conspire to comprise unique environments that enable the catalysis of reactions with unparalleled efficiency and specificity.[1] In the past few decades, our ability to obtain molecular structures of proteins and perform site-directed mutagenesis has generated valuable insights into how enzymes carry out their functions at the atomic level.[2−5] These studies often focused on the role of catalytic residues that perform the chemistry, including general acid/base, covalent, and electrostatic contributions to catalysis.[6,7] However, studies that systematically address the contributions of all active-site residues not directly involved in bond making and breaking are rare.[5,8,9] In addition, these noncatalytic amino acids are routinely assumed to be only important for facilitating substrate binding. Some previous studies have shown that these residues could be as essential to the enzyme's function as catalytic residues.[8,9] The active-site microenvironment created by amino acids not directly involved in bond making/breaking enables enzymes to enhance catalysis through a variety of strategies, such as introducing strain to destabilize the substrate and preorganizing active-site dipoles for transition-state stabilization.[10−13] Our understanding of how nature utilizes residues beyond those directly involved in the reaction chemistry to enhance enzyme efficiency is of paramount importance to enzyme engineering and design. Here, we analyze the active-site residues in L-threonine dehydrogenase to assess how they individually and collectively contribute toward substrate binding and catalysis alongside previously recognized catalytic residues. An improved understanding on this enzyme will also provide a platform to develop novel biocatalysts that can perform selective oxidation of β-amino alcohols to produce its activated carbonyl products for synthetic applications.[14,15]

The enzyme used in this work is L-threonine dehydrogenase derived from *Thermoplasma volcanium* (tvTDH). This enzyme catalyzes the oxidation of β-alcohol on L-threonine to a ketone with nicotinamide adenine dinucleotide (NAD^+) serving as the oxidizing agent (Figure 1). This function is essential to amino acid catabolism pathways, in which tvTDH initiates the degradation of L-threonine by oxidizing it to 2-amino-3-ketobutyrate that is subsequently deacetylated by ketobutyrate-CoA ligase to glycine.[16] Extensive structural analysis of this enzyme has been performed, resulting in multiple crystal structures with various bound ligands (PDB IDs: 3AJR, 3A4V,

Received: April 26, 2017
Accepted: June 20, 2017
Published: July 7, 2017

DOI: 10.1021/acsomega.7b00519
ACS Omega 2017, 2, 3308−3314

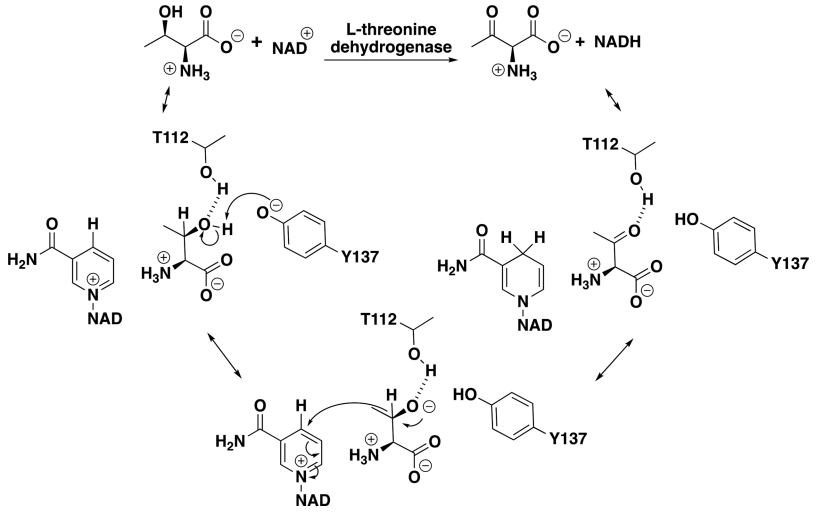

Figure 1. Schematic of the tvTDH reaction. L-Threonine dehydrogenase catalyzes the oxidation of β-alcohol to form 2-amino-3-oxobutanoic acid with the reduction of NADH. The proposed reaction mechanism consists of the deprotonation of the alcohol by the phenolate of Y137 with T112 stabilizing the oxygen atom to form the ketone.

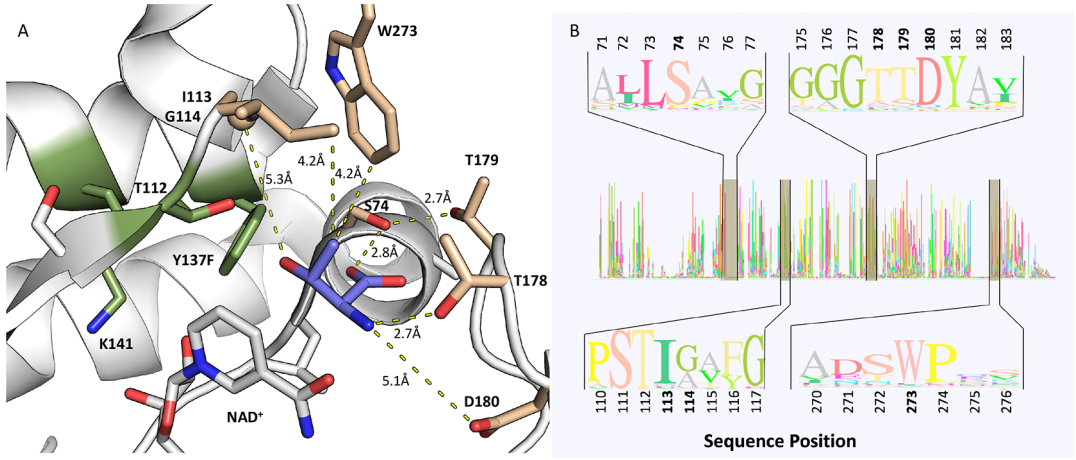

Figure 2. Active-site analysis of tvTDH. (A) Zoom-in view of the active site shows the molecular interactions between tvTDH and L-threonine. The distances between the mutated residues (light brown) to the closest atom on L-threonine are measured and represented with yellow-dotted lines. Residues proposed to be involved in the reaction chemistry are highlighted in green. L-Threonine is highlighted in light purple. (B) Sequence logo of 64 diverse sequences that are homologous to tvTDH. The regions surrounding the mutations tested are highlighted, and their positions in the sequence are shown in bold.

3A9W, and 3A1N).[17] On the basis of the structure with L-threonine bound (PDB ID: 3A9W), the reaction mechanism of this enzyme is proposed to involve Y137, facilitating the deprotonation of β-alcohol on L-threonine, followed by a hydride transfer from β-carbon to the coenzyme NAD^+ (Figure 1).[17] The residue T112 is proposed to be responsible for stabilizing the oxyanion intermediate.[18] A previous study characterized the activity of Y137F, a mutant that results in the inactivation of this enzyme, consistent with the proposed mechanism.[17]

Although residues previously proposed to be directly involved in the reaction chemistry have been analyzed, the importance and role of other residues within the active-site pocket remain elusive. In this work, we systematically mutated seven amino acids that form the reminder of the active-site residues interacting with L-threonine into alanine to quantify the contribution of each side chain toward the catalytic efficiency of enzymes. In addition, we characterized substrate analogs of L-threonine, in which functional groups of the substrate were systematically removed. This analysis of the tvTDH active site enabled us to isolate the role of each individual residue in the context of the proposed mechanism. These mechanistic details improve our understanding of how this enzyme achieves function and should advance our ability to rationally engineer enzymes.

RESULTS AND DISCUSSION

Identification of Relevant Active-Site Residues. The crystal structure of tvTDH with NAD^+ and L-threonine bound (PDB ID: 3A9W) was used to identify residues that have direct contacts with the substrate. All residues having any atoms situated within 6 Å of L-threonine were considered, with the exception of the previously proposed catalytic residues (Y137 and T112) and residues making direct molecular interactions with NAD^+ (defined as within 4 Å of NAD^+; Figure 2A).[17] This analysis resulted in the identification of seven residues that are primarily interacting with L-threonine: S74, I113, G114, T178, T179, D180, and W273 (Figure 2A).

DOI: 10.1021/acsomega.7b00519
ACS Omega 2017, 2, 3308−3314

k_{cat}/K_M ($M^{-1}s^{-1}$)	WT	I113A	G114A	T178A	D180A	W273	S74A	T179A
L-Threonine	6.6E+02	1.1E+02	2.7E+03	3.5E+01	1.1E+01	3.5E-01	2.9E+00	1.6E+00
L-Serine	1.7E-01	5.5E-02	5.4E-01	9.5E-03	N.D.	N.D.	N.D.	N.D.
R-(-)-1-amino-2-propanol	N.D.	N.D	2.3E-02	N.D.	N.D.	N.D.	N.D.	N.D.
L-Threoninol	8.7E-04*	N.D.	3.5E-03	N.D.	N.D.	N.D	3.9E-03	N.D

K_M (M)	WT	I113A	G114A	T178A	D180A	W273	S74A	T179A
L-Threonine	2.6E-03	8.8E-03	5.7E-04	1.1E-02	4.3E-02	N.D.	N.D.	N.D.
L-Serine	6.1E-02	1.8E+00	1.8E-01	1.6E+00	N.D.	N.D.	N.D.	N.D.
R-(-)-1-amino-2-propanol	N.D.	N.D.	3.6E-01	N.D.	N.D.	N.D.	N.D.	N.D
L-Threoninol	N.D.	N.D.	N.D.	N.D.	N.D.	N.D.	N.D.	N.D.

k_{cat} (s^{-1})	WT	I113A	G114A	T178A	D180A	W273	S74A	T179A
L-Threonine	1.7E+00	7.3E-01	1.6E+00	N.D.	3.7E-01	N.D.	N.D.	N.D.
L-Serine	1.0E-02	2.6E-02	1.3E-02	1.4E-02	N.D.	N.D.	N.D.	N.D.
R-(-)-1-amino-2-propanol	N.D.	N.D.	8.5E-03	N.D.	N.D	N.D.	N.D.	N.D.
L-Threoninol	N.D.	N.D.	N.D.	N.D.	N.D.	N.D.	N.D.	N.D.

N.D.	> 3-fold loss of function	Neutral	> 3-fold gain of function

Figure 3. Kinetic characterization. Characterization of kinetic constants of the WT enzyme and alanine mutants on a panel of substrate analogs. The heat map represents the fold changes in k_{cat}, K_M, and $k_{cat}K_M^{-1}$ each mutant has on individual substrates relative to the WT enzyme. Orange represents an improvement (i.e., increase in $k_{cat}K_M^{-1}$ and k_{cat} and decrease in K_M) of at least 3-fold, and blue represents a decrease in $k_{cat}K_M^{-1}$ and k_{cat} and an increase in K_M of at least 3-fold. N.D. indicates k_{cat}, K_M, or $k_{cat}K_M^{-1}$ below the limit of detection. Asterisk indicates samples that were assayed in biological duplicates instead of triplicates.

Amino acid conservation analysis was performed to assess the importance of these seven positions within the tvTDH enzyme family. The crystal structure of L-threonine dehydrogenase (PDB ID: 3A9W) was used as the initial input to a Pfam[19] search to identify its protein family. The enzyme tvTDH is assigned to the NAD-dependent epimerase/dehydratase family with 65846 sequence homologs residing in the clan. To filter out redundant sequences, we processed the results using CD-HIT[20] with a sequence identity cutoff of 80%. Sequences within 10% length of the tvTDH sequence were kept for further analysis. After aligning the remaining sequences using MUSCLE,[21] they were further curated to remove the proteins that do not possess the residues forming the catalytic residues associated with this enzyme function. This series of bioinformatics operations produced a final set of 64 genes for analysis. An examination of the all-to-all sequence identity of these 64 sequences showed that this sequence set possesses overall sequence identities ranging from 17 to 81% with an average of 36%. On the basis of the multiple sequence alignment, the average sequence conservation at each individual site for S74, I113, G114, T178, T179, D180, and W273 is 89, 89, 60, 78, 74, 88, and 91%, respectively (Figure 2B, Table S1). The high level of evolutionary conservation observed for these residues indicates that these residues are important for substrate recognition or catalysis.

Effects of Alanine Mutations on the Activity of L-Threonine. The site-directed alanine mutants were generated using Kunkel mutagenesis.[22] The sequence-verified plasmids generated were transformed into *Escherichia coli* BLR(DE3) for protein expression, and the proteins were produced through autoinduction procedures. The mutant proteins were purified from the resulting cultures with immobilized metal affinity chromatography, which made use of the 6×-His tag that was engineered into the native tvTDH gene (Figure S1, Document S1). On the basis of the quantification of the purified soluble protein, we observed that protein yields for each of the alanine mutants are within 2-fold of wild-type (WT) (Table S7). Once purified, each mutant was kinetically characterized to determine k_{cat}, K_M, and $k_{cat}K_M^{-1}$ by measuring the accumulation of reduced nicotinamide adenine dinucleotide (NADH) at 340 nm using a spectrophotometer.

The four S74A, T179A, W273A, and D180A mutants decrease the catalytic efficiency by 228-, 413-, 1886-, and 60-fold relative to the native enzyme, respectively (Figure 3, Table S2). For the mutants S74A, T179A, and W273A, it is unclear whether the decrease in efficiency was due solely to K_M or both k_{cat} and K_M, as no saturation kinetics are observed for any of these mutants. S74 makes a hydrogen bond to the carboxylic acid of threonine (Figure 2A). W273 occupies a large space in the active site with its indole motif pointing toward the acid and alcohol functional groups on the L-threonine substrate. On the basis of these observed interactions, all of these residues are predicted to be important in positioning the substrate in a catalytically productive orientation, which is further supported

DOI: 10.1021/acsomega.7b00519
ACS Omega 2017, 2, 3308−3314

by the deleterious effect on K_M and $k_{cat}K_M^{-1}$ of mutating them. D180 is located 5.1 Å from the amino group of the L-threonine substrate (Figure 2A). Although this distance is too far to be involved in a direct hydrogen bond, it is well within the distance to have an impact on the substrate through electrostatics or a water-bridged hydrogen bond. The removal of this interaction results in a decrease in $k_{cat}K_M^{-1}$ from 660 to 11 M^{-1} s^{-1}, with a 5-fold decrease in the turnover rate (k_{cat}), from 1.7 to 0.37 s^{-1} and a 16.5-fold increase in K_M, from 2.6 to 43 mM. These observations are consistent with the structure-based hypothesis that the electrostatic effect of the acid is important in stabilizing the ligand in a catalytically competent orientation. Using Eyring's equation (Document S2), free-energy contributions were estimated for S74A, T179A, W273A, and D180A; these estimates indicate that these mutants decrease the catalytic efficiency by 3.2, 3.6, 4.5, and 2.5 kcal mol^{-1}, respectively (Table S6).

The two mutants that were found to have a moderate impact on the catalytic efficiency are I113A, with a 6-fold decrease, and T178A, with an 18-fold decrease in the catalytic efficiency. I113 is observed in the structure to be 4.2 Å from the β-carbon of L-threonine. Given the relatively weak binding associated with the isolated noncovalent hydrophobic interactions, the change of only 6-fold associated with removing this interaction is not surprising. Similarly, T179A is a second-shell mutant and is 2.8 Å from the hydroxyl group of S74, which forms a hydrogen bond with the acid on the L-threonine substrate.

The most unexpected result from this study is associated with the mutant G114A that enhances the catalytic efficiency. G114 is located between the residues I113 and W273, with the Cα carbon being 5.3 Å from the β-alcohol of L-threonine. Mutating G114 to alanine causes a 4-fold increase in the catalytic efficiency, from 660 to 2700 M^{-1} s^{-1}, which breaks down to a 6% decrease in the turnover rate, from 1.7 to 1.6 s^{-1}, and a 4.6-fold decrease in K_M, from 2.6 to 0.6 mM. Although the backbone of this glycine residue is too far to make any hydrogen bond or significant hydrophobic interactions with the substrate, mutating this residue to alanine in PyMOL leads to a distance of about 2.5 Å between the new methyl group and the catalytic residue Y137 (Figure 2A). We hypothesize that this steric clash between G114A and T137 will cause subtle structural rearrangements of the surrounding residues. The 4.6-fold decrease in the observed K_M suggests that this rearrangement could provide an enhancement in binding of the ligand.

Effects of Mutations on Kinetic Constants of Non-Native Substrates. Previous studies have shown that this enzyme is highly specific to L-threonine with no activity on L-serine, L-homoserine, 2-propanol, 1,4-butanediol, 2,3-butanediol, 1,2-propanediol, ethanol, 1-butanol, D-threonine, DL-*allo*-threonine, and DL-*threo*-3-phenylserine.[17] To further analyze the molecular interactions essential for enzyme function, we characterized the kinetic constants of our mutants against a panel of non-native substrates. These substrates were chosen to systematically remove the functional groups of L-threonine to further elucidate whether each individual residue had evolved to interact with a particular part of the L-threonine substrate. The non-native substrates tested are L-serine, (*R*)-(−)-1-amino-2-propanol, (*R*)-3-hydroxybutyric acid, and L-threoninol (Figure 4). Our results show that, contrary to previous reports, the WT enzyme is not completely specific to L-threonine and is active on two of the four tested substrates: L-serine and L-threoninol.[17] The WT enzyme does not have activity on (*R*)-(−)-1-amino-2-propanol, but one mutant, G114, was minimally

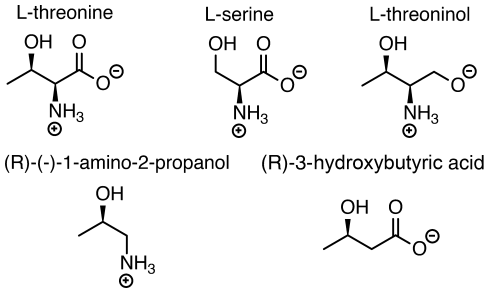

Figure 4. Substrate panel. A series of commercially available substrates each missing a functional group relative to L-theronine were evaluated to determine the importance of each chemical group on the catalytic efficiency.

active (Figure 4). No activity is observed with the native enzyme or any mutant on (*R*)-3-hydroxybutyric acid. However, consistent with previous reports, L-threonine is the preferred substrate, with the four substrates tested here having 3900–760 000-fold lower catalytic efficiency than L-threonine (Figure 3, Tables S2–S5).

Generally, the effect of mutation on L-threonine was similar to that on the non-natural substrate with a few notable exceptions. S74A provides a hydrogen bond interaction to the acid motif on L-threonine. Although L-threoninol has an alcohol group replacing the acid, S74 is expected to provide the same hydrogen bond to the alcohol assuming that the crystal structure substrate conformation was employed. Intriguingly, S74A increases the catalytic efficiency by 4.5-fold, which is opposite to the 220-fold drop observed on L-threonine. The mutant T178A disrupts the hydrogen bond interaction of the residue to the amino moiety on L-threonine and reduces the catalytic efficiency by 413-fold with L-threonine (Figures S2–S5).

Intrinsic Substrate Reactivity. To further rationalize the differences in enzyme activity for the substrates examined, we evaluated their intrinsic hydride-donating abilities. The inherent ability to donate a hydride (gauged by the free energy of the reaction in Figure 5A) was calculated for all five substrates (Figure 5B, Document S3) using Gaussian09[23] at the Solvation Model based on Density (SMD)(water)-B3LYP/6-31+G-(d,p)[24−27] level of theory using the conformation of threonine observed to be bound in the enzyme active site (Figure 2A; PDB ID: 3A9W). In this conformation, the ammonium group is anti to the hydroxyl group in the side chain, and the two moieties cannot form an internal hydrogen bond.

Using L-threonine as the reference point, our calculations show that L-threoninol and L-serine are less willing to donate a hydride ion, by 2.8 and 2.5 kcal mol^{-1}, than is L-threonine (Figure 5B). By contrast, (*R*)-(−)-1-amino-2-propanol and 3-hydroxybutyric acid are 2.2 and 10.8 kcal mol^{-},[1] respectively, which are more willing to donate a hydride to NAD^+ than is L-threonine. These results, along with our experimental kinetic constants, suggest that NAD^+ oxidations of L-threoninol and (*R*)-3-hydroxybutyric acid are chemically possible given a compatible active site, but the inactivity of this enzyme on (*R*)-3-hydroxybutyric acid is likely due to a suboptimal binding orientation. Overall, the lack of a strong correlation between the hydride-donating ability and the observed activity suggests that tvTDH did not evolve to harness the intrinsic substrate reactivity for enzyme catalysis.

DOI: 10.1021/acsomega.7b00519
ACS Omega 2017, 2, 3308−3314

A

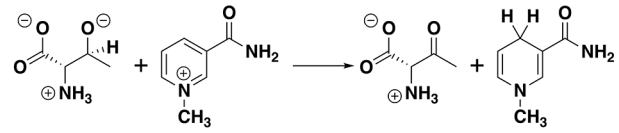

B

Name	Structure	Hydride Donation (kcal/mol)	Relative Donation (kcal/mol)
L-threonine	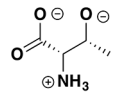	-9.58	0.00
L-threoninol		-6.78	2.79
(R)-(-)-1-amino-2-propanol	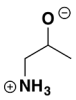	-11.76	-2.19
(R)-3-hydroxybutyric acid	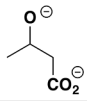	-20.39	-10.82
L-serine	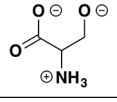	-7.07	2.50

Figure 5. Quantum mechanical evaluation of the intrinsic reactivity. (A) Schematic of molecular transformation used to calculate the hydride affinities for each substrate. (B) Absolute and relative hydride affinities for each of the five substrates.

CONCLUSIONS

Our analysis of tvTDH and its active-site alanine mutants has revealed that the active-site residues examined play varying roles in binding and catalysis on primary and secondary alcohols. This systematic analysis provides understanding of the key features that impart tvTDH enzyme activity beyond the residues directly involved in the enzyme chemistry. In addition, we have shown that this enzyme is capable of utilizing a broader range of substrates than previously reported, albeit at vastly lower levels of catalytic efficiency than observed for threonine. The intricacies revealed here not only increase our fundamental understanding of catalysis by threonine dehydrogenase but also set the stage for future enzyme engineering efforts, in particular, those aimed at modulating the activity to create libraries of redox enzymes capable of reducing β-amino alcohols. Furthermore, systematic studies such as the one presented here are essential for providing the data sets necessary for training energy functions and sampling methods employed in enzyme engineering algorithms.[8]

EXPERIMENTAL SECTION

General Materials. L-Threonine (catalog #: T8625), L-threoninol (catalog #: 469963), (*R*)-(−)-1-amino-2-propanol (catalog #: 238856), (*R*)-3-hydroxybutyric acid (catalog #: 238856), and L-serine (catalog #: S4500) were all purchased from Sigma-Aldrich. β-Nicotinamide adenine dinucleotide hydrate (catalog #: 124530050) was purchased from Acros Organics. All other buffers and reagents were purchased from Sigma-Aldrich or Fisher Scientific. A 96-well plate for kinetic assays was from Fisher Scientific (catalog# 07-200-842).

Mutagenesis, Expression, and Purification of tvTDH. The gene encoding the L-threonine dehydrogenase derived from tvTDH was codon-optimized and synthesized by Thermo Fisher Scientific for expression in *E. coli*. Using Gibson Assembly, it was cloned between the NdeI and XhoI sites in pET29b+. This encoded a C-terminal 6×-His tag to allow for affinity column purification with cobalt resin. The mutagenesis was performed using Kunkel mutagenesis to introduce the mutations in the tvDH gene on Transcriptic using their standard protocol.

Sequence-verified native and mutant plasmids were transformed into chemically competent *E. coli* BLR cells for protein expression. Protein expressions were first observed with the inoculation of transformed cells in 20 mL of growth media (50 μg/mL kanamycin in terrific broth), which were grown for 24 h at 37 °C in 50 mL falcon tubes. The turbid cultures were then centrifuged for 30 min at 4700 rpm. The cell pellets were then resuspended in 20 mL of autoinduction media containing kanamycin (50 μg/mL kanamycin, 1 mM $MgSO_4$, 5052 and NPS from the standard autoinduction media protocol[28]), and proteins were allowed to express for 24 h shaking at 18 °C. The cultures were then harvested by centrifuging for 30 min at 4700 rpm. Pellets were resuspended in 1 mL of lysis buffer containing 1 mg lysozyme, 0.1 mg DNase, 200 μL BugBuster, and 2 mM phenylmethane sulfonyl fluoride (PMSF) and rocked for 30 min at 4 °C. The lysate was then clarified by centrifugation for 30 min at 15 000 rpm. Purification of the supernatant was done with gravity column over 100 μL slurry of cobalt resin and was washed with 5 mL of wash buffer that contains 50 mM *N*-(2-hydroxyethyl)piperazine-*N*′-ethanesulfonic acid (HEPES) (pH 7), 200 mM NaCl, and 5 mM imidazole. The protein was eluted with 0.2 mL of elusion buffer containing 50 mM HEPES (pH 7), 200 mM NaCl, and 200 mM imidazole and was centrifuged at 1000 rpm for 1 min to extract the solution from the bead bed.

Kinetic Experiments. The activity of the WT and tvTDH mutants was measured via the accumulation of NADH as a result of the oxidation of the assayed substrates. The change in absorbance of NADH was measured at a wavelength at 340 nm using BioTek Epoch and Synergy microplate spectrophotometers on a 96-well nonbinding plate.

To establish the limit of detection for the assay, we grew and expressed green fluorescent protein (GFP) as a negative control. We tested for activity with GFP at the highest concentration for each substrate to elucidate the error caused by detection limits and contamination. There was no activity with GFP for L-threonine, L-serine, and L-threoninol but trace activity with (*R*)-3-amino propanol. We determined any activity on (*R*)-3-amino-propanol within 3-fold of the trace activity observed to be inactive.

The assay of the WT and mutants on the native substrate was performed by a threefold serially diluted substrate in a 100 μL reaction containing 10 mM NAD^+, 200 mM glycine (pH 10), and 200 mM NaCl. The initial concentration for WT and each mutant was chosen based on producing an accurate Michaelis–Menten curve (Figures S2–S5). The initial concentration of the L-threonine activity assay for WT and T179A was 20 mM and was serially diluted threefold to obtain the various concentrations tested. The initial concentration of L-threonine used for I113A, W273A, D180A, and S74A was 100 mM and was serially diluted threefold. The initial concentration of L-threonine for T178A and G114A was 40 and 5 mM, respectively, and was serially diluted threefold. The numbers

DOI: 10.1021/acsomega.7b00519
ACS Omega 2017, 2, 3308–3314

reported are the average of three biological replicates, and the error is the standard deviation between them. The data that have an asterisk are calculated with biological duplicates. The assay was performed at room temperature or 25 °C.

The assay of the WT and mutants on non-native substrates L-serine, L-threoninol, and (*R*)-(−)-1-amino-2-propanol was performed by a fourfold serially diluted substrate starting at 1 M concentration of the substrate in 100 μL reaction containing 200 mM glycine (pH 10), 200 mM NaCl, and 10 mM NAD^+. The enzymes were undiluted in all assays on non-native substrates.

Quantum Mechanics Calculations. QM calculations were performed with Gaussian09.[21] Minima were located using B3LYP/6-31+G(d,p)[22−25] with the SMD continuum solvation approach using water. All calculations were conducted without any protein present. Stationary points were confirmed as minima using harmonic vibrational analysis (no imaginary frequencies for minima). Structures and energies used for calculations are provided in Supporting Information.

■ ASSOCIATED CONTENT

Supporting Information

The Supporting Information is available free of charge on the ACS Publications website at DOI: 10.1021/acsomega.7b00519.

SDS-PAGE gel, Michaelis−Menten curve fits, L-threonine dehydrogenase family active-site amino acid profile, kinetic constants, ΔΔ*G*, first-order Arrhenius equations, and results of proton affinity calculations (PDF)

Structures and energies used for calculations (ZIP)

■ AUTHOR INFORMATION

Corresponding Author

*E-mail: jbsiegel@ucdavis.edu (J.B.S.).

ORCID

Morgan Desjardins: 0000-0002-9772-451X

Dean J. Tantillo: 0000-0002-2992-8844

Notes

The authors declare no competing financial interest.

■ ACKNOWLEDGMENTS

We are grateful for the funding and support from UC Davis, and ARPA-E DE-AR0000429.

■ REFERENCES

(1) Tawfik, D. S. Accuracy-rate tradeoffs: how do enzymes meet demands of selectivity and catalytic efficiency? *Curr. Opin. Chem. Biol.* **2014**, *21*, 73−80.

(2) Zaidi, Z. H.; Smith, D. L. *Protein Structure−Function Relationship*; Springer, 1996.

(3) Bolduc, J. M.; Dyer, D. H.; Scott, W. G.; Singer, P.; Sweet, R. M.; Koshland, D.; Stoddard, B. L. Mutagenesis and Laue structures of enzyme intermediates-Isocitrate dehydrogenase. *Science* **1995**, *268*, 1312.

(4) Schwans, J. P.; Sunden, F.; Lassila, J. K.; Gonzalez, A.; Tsai, Y.; Herschlag, D. Use of anion−aromatic interactions to position the general base in the ketosteroid isomerase active site. *Proc. Natl. Acad. Sci. U.S.A.* **2013**, *110*, 11308−11313.

(5) Sunden, F.; Peck, A.; Salzman, J.; Ressl, S.; Herschlag, D. Extensive site-directed mutagenesis reveals interconnected functional units in the alkaline phosphatase active site. *eLife* **2015**, *4*, No. e06181.

(6) Zhang, X.; Houk, K. N. Why enzymes are proficient catalysts: beyond the Pauling paradigm. *Acc. Chem. Res.* **2005**, *38*, 379−385.

(7) Warshel, A.; Sharma, P. K.; Kato, M.; Xiang, Y.; Liu, H.; Olsson, M. H. Electrostatic basis for enzyme catalysis. *Chem. Rev.* **2006**, *106*, 3210−3235.

(8) Carlin, D. A.; Caster, R. W.; Wang, X.; Betzenderfer, S. A.; Chen, C. X.; Duong, V. M.; Ryklansky, C. V.; Alpekin, A.; Beaumont, N.; Kapoor, H. Kinetic Characterization of 100 Glycoside Hydrolase Mutants Enables the Discovery of Structural Features Correlated with Kinetic Constants. *PLoS One* **2016**, *11*, No. e0147596.

(9) Lucas, J. E.; Siegel, J. B. Quantitative functional characterization of conserved molecular interactions in the active site of mannitol 2-dehydrogenase. *Protein Sci.* **2015**, *24*, 936−945.

(10) Wu, N.; Mo, Y.; Gao, J.; Pai, E. F. Electrostatic stress in catalysis: structure and mechanism of the enzyme orotidine monophosphate decarboxylase. *Proc. Natl. Acad. Sci. U.S.A.* **2000**, *97*, 2017−2022.

(11) Hokenson, M. J.; Cope, G. A.; Lewis, E. R.; Oberg, K. A.; Fink, A. L. Enzyme-induced strain/distortion in the ground-state ES complex in β-lactamase catalysis revealed by FTIR. *Biochemistry* **2000**, *39*, 6538−6545.

(12) Huskey, S. E. W.; Huskey, W. P.; Lu, A. Y. H. Contributions of thiolate "desolvation" to catalysis by glutathione S-transferase isozymes 1-1 and 2-2: evidence from kinetic solvent isotope effects. *J. Am. Chem. Soc.* **1991**, *113*, 2283−2290.

(13) Warshel, A. Multiscale modeling of biological functions: from enzymes to molecular machines (Nobel Lecture). *Angew. Chem., Int. Ed.* **2014**, *53*, 10020−10031.

(14) Yang, Y.; Wahler, D.; Reymond, J.-L. β-Amino Alcohol Properfumes. *Helv. Chim. Acta* **2003**, *86*, 2928−2936.

(15) De Luca, L.; Giacomelli, G.; Porcheddu, A. A very mild and chemoselective oxidation of alcohols to carbonyl compounds. *Org. Lett.* **2001**, *3*, 3041−3043.

(16) Marcus, J. P.; Dekker, E. E. Threonine formation via the coupled activity of 2-amino-3-ketobutyrate coenzyme A lyase and threonine dehydrogenase. *J. Bacteriol.* **1993**, *175*, 6505−6511.

(17) Yoneda, K.; Sakuraba, H.; Araki, T.; Ohshima, T. Crystal structure of binary and ternary complexes of archaeal UDP-galactose 4-epimerase-like l-threonine dehydrogenase from *Thermoplasma volcanium*. *J. Biol. Chem.* **2012**, *287*, 12966−12974.

(18) Berthold, C. L.; Gocke, D.; Wood, M. D.; Leeper, F. J.; Pohl, M.; Schneider, G. Structure of the branched-chain keto acid decarboxylase (KdcA) from *Lactococcus lactis* provides insights into the structural basis for the chemoselective and enantioselective carboligation reaction. *Acta Crystallogr., Sect. D: Biol. Crystallogr.* **2007**, *63*, 1217−1224.

(19) Finn, R. D.; Coggill, P.; Eberhardt, R. Y.; Eddy, S. R.; Mistry, J.; Mitchell, A. L.; Potter, S. C.; Punta, M.; Qureshi, M.; Sangrador-Vegas, A.; Salazar, G. A.; Tate, J.; Bateman, A. The Pfam protein families database: towards a more sustainable future. *Nucleic Acids Res.* **2016**, *44*, D279−D285.

(20) Fu, L.; Niu, B.; Zhu, Z.; Wu, S.; Li, W. CD-HIT: accelerated for clustering the next-generation sequencing data. *Bioinformatics* **2012**, *28*, 3150−3152.

(21) Edgar, R. C. MUSCLE: multiple sequence alignment with high accuracy and high throughput. *Nucleic Acids Res.* **2004**, *32*, 1792−1797.

(22) Kunkel, T. A.; Roberts, J. D.; Zakour, R. A. Rapid and efficient site-specific mutagenesis without phenotypic selection. *Methods Enzymol.* **1987**, *154*, 367−382.

(23) Frisch, M.; Trucks, G.; Schlegel, H.; Scuseria, G.; Robb, M.; Cheeseman, J.; Scalmani, G.; Barone, V.; Mennucci, B.; Petersson, G. *Gaussian 09*, Revision D.01; Gaussian, Inc.: Wallingford CT, 2009.

(24) Becke, A. D. A new mixing of Hartree−Fock and local density-functional theories. *J. Chem. Phys.* **1993**, *98*, 1372−1377.

(25) Becke, A. D. Density-functional thermochemistry. III. The role of exact exchange. *J. Chem. Phys.* **1993**, *98*, 5648−5652.

(26) Marenich, A. V.; Cramer, C. J.; Truhlar, D. G. Universal solvation model based on solute electron density and on a continuum model of the solvent defined by the bulk dielectric constant and atomic surface tensions. *J. Phys. Chem. B* **2009**, *113*, 6378−6396.

(27) Stephens, P. J.; Devlin, F. J.; Chabalowski, C. F.; Frisch, M. J. Ab initio calculation of vibrational absorption and circular dichroism

DOI: 10.1021/acsomega.7b00519
ACS Omega 2017, 2, 3308−3314

spectra using density functional force fields. *J. Phys. Chem.* **1994**, *98*, 11623−11627.
(28) Studier, F. W. Protein production by auto-induction in high-density shaking cultures. *Protein Expression Purif.* **2005**, *41*, 207−234.

DOI: 10.1021/acsomega.7b00519
ACS Omega 2017, 2, 3308−3314